

In-silico Studies of Phytochemicals from Selected Medicinal Plants against Lung Cancer Receptor

Surya Pratap Gurjar¹, Arpita Roy^{1,*} , Aaryan Gupta¹, Vaseem Raja², Sarvesh Rustagi³, Devvret Verma⁴, Swetha Raj⁵

¹ Department of Biotechnology, School of Engineering and Technology, Sharda University, Greater Noida, U.P., India

² Department of Biotechnology, University Centre for Research and Development, Chandigarh University Gharuan, Mohali, Punjab 140413, India

³ School of Applied and Life Sciences, Uttaranchal University Dehradun, Uttarakhand, India

⁴ Department of Biotechnology, Graphic Era Deemed to be University, Dehradun, Uttarakhand, India

⁵ Center for Global Health Research, Saveetha Medical College and Hospitals, Saveetha Institute of Medical and Technical Sciences (SIMATS), Chennai, India

* Correspondence: arbt2014@gmail.com (A.R.);

Scopus Author ID 57672913100

Received: 21.02.2024; Accepted: 8.07.2024; Published: 15.02.2025

Abstract: Lung cancer is a severe illness that often leads to a decline in the quality of life and high rates of mortality and morbidity. In search of effective therapies with minimal side effects, herbal medicines have emerged as a promising option and a significant source of new drugs. The purpose of this study is to explore the potential of *Berberis aristata*, *Bacopa Monnieri*, *Picrorhiza kurroa*, and *Taraxacum officinale* and other living organisms in treating lung cancer by examining their anti-tumor properties using *in-silico* studies. This study demonstrates the abundant potential of plant-based natural products in developing herbal medicines or biologically active compounds to combat cancer. Many experimental findings indicate that medicinal plants and their constituents could positively affect lung cancer. This study found that Berbamine from *Berberis aristata*, Luteolin from *Bacopa Monnieri*, Cucurbitacin D from *Picrorhiza kurroa*, and α -amyrin from *Taraxacum officinale* have the potential to inhibit the 4ZXT receptor and their binding energies are -8.04 , -7.28 , -7.78 and -9.02 kcal/mol. However, it is important to consider each plant's pharmacodynamics and pharmacokinetics limitations.

Keywords: lung cancer; medicinal plants; ERK 2; catechol.

© 2025 by the authors. This article is an open-access article distributed under the terms and conditions of the Creative Commons Attribution (CC BY) license (<https://creativecommons.org/licenses/by/4.0/>).

1. Introduction

Lung cancer develops in lung tissues, disrupting normal cell division and leading to abnormal, uncontrolled growth into a tumor mass. It can invade surrounding tissues and organs, like lymph nodes, and spread to other body parts like the brain and liver [1]. It is the leading cause of cancer-related deaths worldwide, with over a million diagnosed cases annually. Common symptoms of advanced lung cancer include pain, shortness of breath, coughing up blood, cancer that spreads to other parts of the body, and fluid in the chest. Risk factors for lung cancer include exposure to second-hand smoke, radon gas, asbestos, workplace carcinogens, and a family history of the disease [2]. Smoking also significantly increases your risk of developing lung cancer. Screening for lung cancer involves testing asymptomatic high-risk individuals to detect cancer early. Biopsy, sputum cytology, and imaging tests are used to confirm the presence of cancer cells. According to NCCN (National Comprehensive Cancer Network) recommendations, biomarker testing is to be done as it includes testing genes or their

products (proteins) within cancer cells, as lung cancer can differ between people by which genes are present. Metastatic lung cancers can be cured energetically through biomarker testing [3].

EGFR (epidermal growth factor receptor) is a surface receptor protein—mutations in the gene that controls EGFR cause the receptors to be overactive. EGFR mutation testing is recommended for metastatic lung adenocarcinomas, large-cell lung carcinomas, and unknown subtypes. Testing may be considered for metastatic squamous cell carcinomas with mixed histology or those who never smoked. A tissue or blood sample can be used for testing [4].

One of the triggers for certain types of lung cancer is the fusion of an ALK gene with EML4. This fusion of ALK-EML4 leads to an overactive ALK receptor on the surface of cells, which can encourage the growth of cancerous cells. ALK testing can be carried out to identify specific subtypes of lung cancer [5]. However, it's important to note that ALK rearrangements are typically not associated with ROS1, EGFR, or KRAS mutations. Therefore, it's essential to consider other factors that may contribute to lung cancer development [6].

Table 1. Classification of plants.

Plant	Kingdom	Family	Genus
<i>Berberis aristata</i>	Plantae	Berberidaceae	<i>Berberis</i>
<i>Bacopa monnieri</i>	Plantae	Plantaginaceae	<i>Bacopa</i>
<i>Picrorhiza kurroa</i>	Plantae	Plantaginaceae	<i>Picrorhiza</i>
<i>Taraxacum officinale</i>	Plantae	Asteraceae	<i>Taraxacum</i>

Berberis aristata, commonly known as the Indian Barberry or Daruharidra, is a perennial shrub growing up to 5 meters in height (Table 1). This shrub is notable for its attractive reddish-brown stems and branches, which make it visually appealing, in addition to its medicinal properties. The leaves of *Berberis aristata* are slightly leathery with an obovate or narrowly elliptic blade, contributing to the plant's resilience in various environmental conditions [7]. The flowers of the Indian Barberry are particularly striking, arranged in stalked panicle-like racemes that measure between 4 to 6 cm in length. Each raceme contains 10 to 20 flowers, adding to the plant's aesthetic and ecological value. The flowers eventually give way to greenish-purple berries that mature into dark purple or black hues. These berries are safe to eat and rich in vitamin C, making them a valuable nutritional resource. *Berberis aristata* is predominantly found in the Himalayas, southern Tibet, and central India, thriving at altitudes ranging from 1300 to 3400 meters. This wide range indicates the plant's adaptability to various climatic conditions [8]. The flowering period typically occurs between April and June, when the plant is most vibrant and active. One of the key medicinal properties of *Berberis aristata* lies in its ability to treat skin conditions, such as psoriasis and inflammation, due to its potent anti-inflammatory and anti-psoriatic properties. The active compounds in the plant, including berberine, have been shown to reduce inflammation and modulate the immune response, which can alleviate the symptoms of psoriasis.

Additionally, *Berberis aristata* serves several other therapeutic roles [9]. It acts as a cholagogue, stimulating the flow of bile from the liver, which aids in digestion and detoxification. As a stomachic, it helps improve appetite and digestive function. Its laxative properties assist in relieving constipation, while its diaphoretic effects promote sweating, which can help detoxify the body and manage fevers. The numerous health benefits of *Berberis aristata* are attributed to its rich phytochemical composition. It contains alkaloids, especially berberine, the primary bioactive compound responsible for its therapeutic effects. Berberine

has been extensively studied for its antimicrobial, anti-inflammatory, and antioxidant properties, making it a valuable component in herbal medicine [10].

Bacopa monnieri, commonly referred to as water hyssop, is a creeping marsh plant that has been a staple in Ayurvedic medicine for centuries due to its reputed cognitive-enhancing and mood-related benefits (Table 1). This herb has recently garnered scientific attention for its potential effects on memory and cognition [11]. Some studies suggest that *Bacopa monnieri* might contribute to slight improvements in memory, although these effects are not universally consistent across different tests and populations. For instance, a 2014 meta-analysis of randomized controlled trials indicated that *Bacopa monnieri* could enhance cognition, particularly by improving attention speed. However, a more recent 2021 meta-analysis did not find significant clinical differences in nootropic (cognitive-enhancing) or mood-related outcomes [12]. The variability in study results leaves the overall evidence for *Bacopa monnieri's* efficacy inconclusive. *Bacopa monnieri's* cognitive benefits may be attributed to its interaction with various neurotransmitter systems, including dopamine, serotonin, and cholinergic. One notable effect of *Bacopa* is its potential to promote neuronal communication through the growth of dendrites, which are the branches of neurons that facilitate intercellular communication. This dendritic growth can enhance the connectivity between brain cells, potentially improving cognitive functions.

Additionally, *Bacopa monnieri* is rich in antioxidants, such as flavonoids and saponins, which help reduce oxidative stress and protect cells from damage. These antioxidant properties play a crucial role in maintaining overall brain health by mitigating the effects of harmful free radicals. Preliminary research also hints at *Bacopa's* potential mood-related benefits. Some studies suggest that it may have antidepressant and anxiolytic effects, possibly by reducing cortisol secretion and preventing the depletion of dopamine and serotonin during periods of chronic stress. These effects could help stabilize mood and reduce anxiety levels.

Picrorhiza species, a small perennial plant, is well-adapted to cool and moist climates. This plant thrives in porous sandy clay-textured soil, which allows the rhizomes to spread horizontally beneath the surface (Table 1). From these rhizomes, aerial sprouts emerge at the nodes, contributing to the plant's growth and propagation [16]. The leaves of *Picrorhiza* are characterized by their sharp, serrated edges, and they turn black when dried, a distinctive feature that aids in identifying the plant. This species predominantly grows in the alpine regions of the Himalayas, extending from Kashmir to Sikkim, at altitudes ranging between 3000 to 4500 meters. It is typically found in moist environments near springs and on moist rocks, where the conditions are ideal for its growth. The plant displays variation in its leaf morphology depending on the altitude: the narrow-leaf variety thrives in higher alpine regions, while the broad-leaf variety is found at lower altitudes under shrubs in moist conditions with high humus content [17]. The flowers of *Picrorhiza* are small and come in shades of white or pale blue-purple. These flowers are arranged in dense terminal spikes, which are clusters at the end of the plant's stem. Each flower spike is accompanied by bracts that are oblong or lanceolate and equal in length to the calyx, the outer floral envelope. The sepals of the flowers are also lanceolate, contributing to the plant's characteristic appearance. Following the flowering phase, the plant produces fruit, a two-celled spherical capsule. This capsule contains numerous white seeds, each with an oblong curved raphae, a ridge that runs along the seed's surface [18]. The flowering and fruiting period for *Picrorhiza* typically occurs from June to August, aligning with the summer months in the Himalayan regions. One of the most significant derivatives of *Picrorhiza* is Kutki, a herbal medicine with a wide range of therapeutic properties. Kutki is

renowned for its antipyretic (fever-reducing) properties, making it useful in managing fevers. It also serves as an anthelmintic, helping to expel parasitic worms, and as a carminative, relieving flatulence. As a stomachic, Kutki improves appetite and stimulates gastric secretions, aiding digestion. Its hepatoprotective qualities make it valuable in protecting the liver and managing liver-related conditions [19].

The dandelion, scientifically known as *Taraxacum officinale*, is a herbaceous plant that is native to various regions across North America, Europe, and Asia. It has been extensively utilized in traditional medicine owing to the rich assortment of phytochemicals present in its roots, leaves, and flowers. These phytochemicals contribute to the plant's numerous health benefits, which include diuretic, anti-inflammatory, and antioxidant properties [20]. The dandelion is easily recognizable by its bright yellow flower heads, which consist of numerous tiny florets. These flower heads undergo a fascinating transformation, turning into silver-tufted balls that disperse their seeds through the wind, aiding in the widespread propagation of the plant. This wind dispersal mechanism is facilitated by the plant's seeds, known as achenes, each attached to a pappus, a tuft of fine hairs that acts like a parachute. Dandelions can grow up to 70 cm (about 27.5 inches) tall. The plant features leafless stems that are hollow and produce a milky latex when broken. These stems hold the flower heads aloft, often at a height equal to or greater than the surrounding foliage [21]. The leaves of the dandelion are quite variable in size, ranging from 5 to 45 cm (2 to 18 inches) in length and 1 to 10 cm (0.4 to 4 inches) in width. They are typically lobed or toothed, with the margins of the leaves featuring sharp or dull teeth, giving the plant a distinctive appearance. Its roots, for instance, are commonly used to support liver health and stimulate bile production, which aids in digestion. The leaves are well-known for their diuretic properties, which help in promoting urine production and eliminating excess water from the body [22]. Dandelion leaves are also a rich source of vitamins A, C, and K and minerals like iron, calcium, and potassium, making them a nutritious addition to salads and other culinary dishes. The flower heads of the dandelion contain antioxidant compounds that help neutralize free radicals, potentially reducing the risk of chronic diseases. These flowers are sometimes used to make dandelion wine or infused in oils for various therapeutic purposes. Additionally, the entire plant has been employed in traditional remedies to treat various ailments, such as digestive disorders, skin issues, and inflammation [23].

Computational biology is a field of biology that uses computer-based techniques to analyze and interpret biological data. It is an essential tool in molecular docking, as it allows researchers to predict how a small molecule will interact with a target protein based on its chemical and structural properties. Molecular docking is a computational technique used to predict the binding of small molecules, such as drugs or natural compounds, to a target protein [24]. It is an essential tool in drug discovery and development, as it allows researchers to identify potential drug candidates that may have therapeutic effects in treating various diseases, including lung cancer. Molecular docking and computational biology can predict the binding affinity of a small molecule to a target protein, which measures how tightly the two molecules will bind to each other. This information is critical in identifying potential drug candidates that may have therapeutic effects in the treatment of lung cancer [25].

2. Materials and Methods

2.1. Selection of the target.

The structure of the Complex of ERK2 with catechol (PDB: 4ZXT) was selected from the RCSB Protein Data Bank database. The extracellular signal-regulated kinase 2 (ERK2) is a crucial component of the RAS/RAF/MEK/ERK signaling pathway. In lung cancer, ERK2 is constitutively activated, making it an attractive therapeutic target. Catechol, a natural small molecule, inhibits ERK2 kinase activity by directly binding to its active site. This interaction disrupts the ERK2/c-Myc signaling axis, reducing tumor growth in vitro and in vivo. The crystal structure of the ERK2-catechol complex (PDB: 4ZXT) serves as a valuable starting point for computational studies to identify synthetic inhibitors for lung cancer treatment [26].

2.2. Selection of ligand.

The compound database was used to prepare the chemical structure of phytochemicals from *Berberis aristata*, *Bacopa Monnieri*, *Picrorhiza kurroa*, and *Taraxacum officinale* with the help of the ChemDraw online tool [27].

2.3. Target and ligand optimization.

During docking analysis, the phytochemicals and target protein coordinates were optimized for stable conformation and minimum energy [28].

2.4. Bioavailability radar.

Analyzation of drug likeliness of various cannabinoids with binding energy less than the control one. After that, we consider six properties and form a bioavailability radar using the SwissADME tool. Solubility, size, lipophilicity, polarity, flexibility, and saturation are the six parameters that we consider.

It provides a graphical representation of the predicted bioavailability profile of a compound based on its physicochemical properties. By plotting key parameters such as molecular weight, lipophilicity, aqueous solubility, gastrointestinal absorption, and permeability on the radar plot, the bioavailability radar enables researchers to assess a compound's drug-likeness and potential oral absorption [29]. It helps identify potential issues affecting bioavailability, allowing researchers to prioritize optimization efforts. Additionally, the radar plot facilitates the comparison of multiple compounds, enabling the assessment and selection of candidates with more favourable bioavailability profiles. The Bioavailability Radar guides the optimization of drug properties by exploring the impact of changes on bioavailability parameters, aiding in improving drug efficacy and delivery. Overall, the Bioavailability Radar in the SWISS ADME tool is a valuable asset in drug analysis, assisting researchers in making informed decisions during drug development and design processes [30].

2.5. Molecular docking studies.

In drug discovery, molecular docking is a computational procedure used to predict the orientation of a ligand to its macromolecular target to form a stable complex. Autodock 4.2 is open-source software that performs docking studies and uses an empirical scoring function to calculate the binding affinity of the protein-ligand complex [31]. Active compounds are

inserted into the active site pockets of extracellular signal-related kinase 2 (ERK2), a crucial target for lung cancer drugs, to understand interactions between ligands and targets better. The PDB ID for this protein target is 4ZXT [32]. The macromolecule underwent a process wherein water molecules were removed, and polar hydrogens were added [33]. Sketches of the ligands were created using Chemsketch and saved in MDL file format. The ligand energies were minimized and converted to PDBQT format using PyRx [34]. The active site of the target molecules was identified. A 3D grid box was set up to cover the target molecule's active site for molecular docking. The conformation with the lowest binding energy was determined to have the highest docking score [35].

3. Results and Discussion

A recent study found that the methanolic extract from *B. aristata* demonstrated significant anticancer effects in human osteosarcoma cells (HOS). This was achieved through the induction of ROS generation, enhanced apoptosis, nuclear fragmentation, autophagy, and caspase-3 activity. The extract also reduced cell viability, whether used alone or combined with other treatments [36]. One of the studies was to develop a new form of *Berberis aristata* extract that could potentially be used to treat tumors. Gelatin lipid-Nano carriers loaded with the extract were created using a double emulsion solvent evaporation method and were characterized using different techniques. The resulting particles were found to have a hydrodynamic diameter of 322 ± 7 nm, a zeta potential of -31.49 ± 4.85 mV, and a polydispersity index of 0.397 ± 0.102 mV. The extract was efficiently entrapped within the particles and demonstrated effective cytotoxicity against MCF-7 cells in vitro. Apoptotic bodies were observed, indicating that the cytotoxicity was due to apoptosis. In-vivo analysis in female mice showed that the extract was comparable to cisplatin in reducing tumor volume. On the 10th day, the GLN-BA (10 mg/kg) reduced the tumor volume to $35 \pm 11\%$, while cisplatin (3 mg/kg) reduced it to $41 \pm 5\%$ [37].

Another study was to assess the potential anticancer properties of a mixture of Polish propolis extract (PPE) and extracts derived from commercial products of *Bacopa monnieri*. Previous studies have not explored the combined effects of PPE and *Bacopa* extracts, especially in glioblastoma cell lines. Our research is the first to provide evidence for the beneficial use of this combination in treating such cells [38]. Another study states that *Bacopa monnieri* contains multitudes of distinct bioactive phytoconstituents having numerous benefits that can be exploited for the therapeutic intervention of various neuropathological disorders. The study on molecular binding suggests that Luteolin specifically binds to the DNA gyrase binding site, making it a potential antimicrobial agent. Luteolin may exert its biological activities through various mechanisms, including modulation of ROS levels, inhibition of topoisomerases I and II, reduction of NFkappaB and AP-1 activity, stabilization of p53, and inhibition of PI3K, STAT3, IGF1R, and HER2 [39].

Research suggests that *P. kurroa* extracts and components may be beneficial in protecting against cancer through various cellular and molecular processes. Flavonoids, such as apocynin, found in the plant's rhizome, are believed to contribute to its anticancer properties. A study analyzed the antineoplastic and antioxidant properties of methanolic and aqueous extracts of *P. kurroa* rhizomes on human breast carcinoma, human hepatocellular carcinoma, and human prostate cancer. The extracts were shown to induce apoptosis in all three cell lines examined. Picroliv was also found to be a promising agent for reducing injury following chemotherapy and radiation. Plant extracts have demonstrated cytotoxic and antioxidant

properties that could aid in fighting cancer. Studies on mice have shown that Picroliv effectively reduces the metastasis and angiogenesis of cancer cells, making it a potential option for cancer treatment [40].

A recent study has suggested that *Taraxacum officinale*, commonly known as the dandelion plant, has the potential to impede specific cellular pathways that facilitate growth and proliferation. This discovery has raised the possibility of utilizing the plant extract as an herbal medication for breast cancer in humans. However, further evaluation and research are necessary to confirm the effectiveness and safety of this treatment option [41]. A recent study discovered that *Taraxacum officinale* can reduce lung W/D ratio, protein concentration, and the number of neutrophils in the BALF after an LPS challenge within 24 hours. It also reduces MPO activity and increases SOD activity in the lungs.

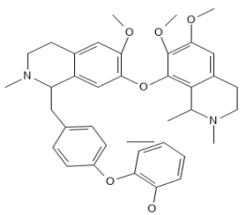
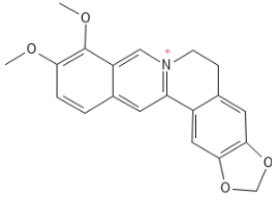
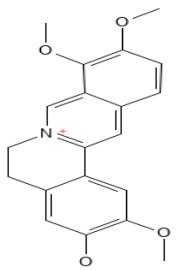
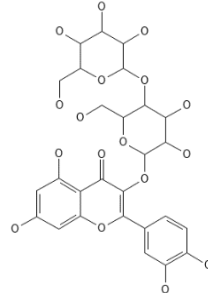
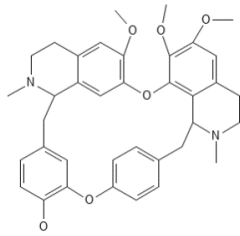
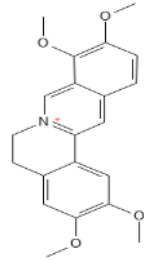
Additionally, the study showed that *Taraxacum officinale* lessened tissue injury in LPS-induced ALI based on histopathological examination. Furthermore, *Taraxacum officinale* also inhibited the production of inflammatory cytokines TNF- α and IL-6 in the BALF 6 hours after LPS challenge in a dose-dependent manner. These findings indicate that *Taraxacum officinale* can protect against LPS-induced ALI in mice [42].

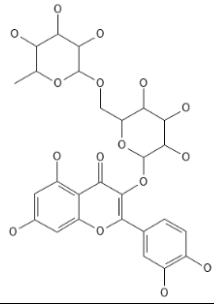
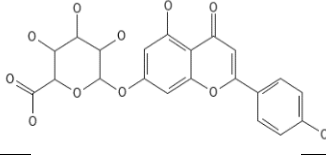
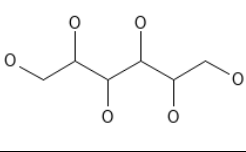
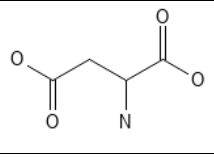
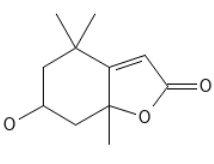
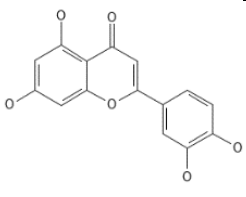
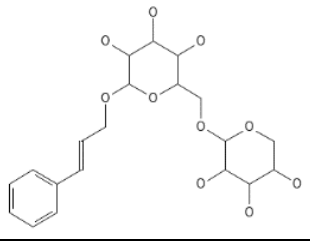
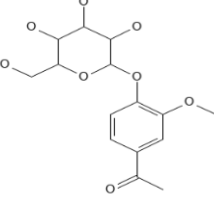
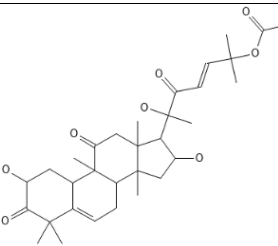
Molecular docking was used to evaluate drug binding strength with the anti-tumor active site of ERK2 and catechol (PDB: 4ZXT) complex. Past research on the ERK2-catechol complex aimed at how the protein and small molecule bind together. Techniques such as X-ray crystallography and nuclear magnetic resonance (NMR) spectroscopy were utilized to precisely determine the arrangement of atoms in the complex and analyze the structural specifics of the binding site. In this study, we have utilized 7 phytocompounds from *Berberis aristata*, 6 phytocompounds from *Bacopa Monnieri*, 10 phytocompounds from *Picrorhiza kurroa*, and 8 phytocompounds from *Taraxacum officinale*.

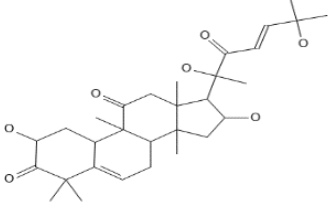
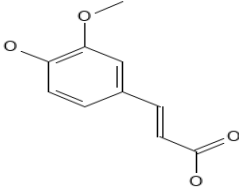
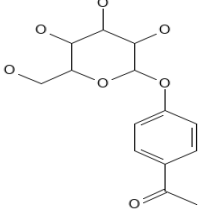
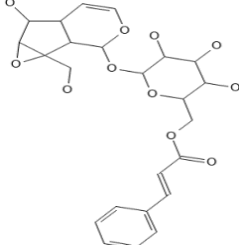
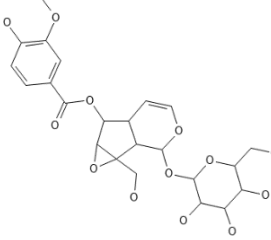
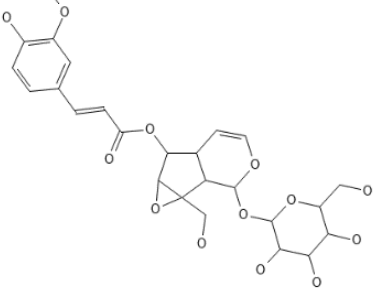
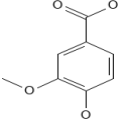
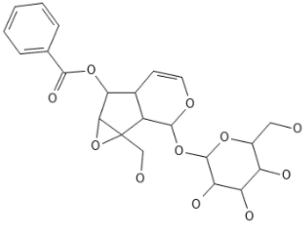
3.1. ADME analysis test.

The study of pharmacokinetics (PK) involves understanding how a drug moves throughout the body, which provides valuable information about how the drug affects the body over time. On the other hand, pharmacodynamics (PD) refers to what the drug does to the body and the resulting pharmacologic response when it reaches the site of action. The processes of absorption, distribution, metabolism, and excretion, collectively known as ADME, describe how a drug moves through and is processed by the body. Understanding a drug's ADME properties is crucial for safe and effective pharmacotherapy development [43]. The 2D structures were obtained with ChemDraw help, provided in Table 1. The computed physicochemical properties of the screened compounds are showcased in Table 2. In *Berberis aristata*, out of seven compounds, three showed no violations, while two had one violation each, and the other two had three violations each. In *Bacopa Monnieri*, out of six compounds, two showed no violations, while three had one violation each, and the other one had two violations. In *Picrorhiza kurroa*, out of ten compounds, three compounds showed no violations, while five showed one violation each, and the other two had three violations each (Table 3). In *Taraxacum officinale*, out of eight compounds, three compounds showed no violations, while three had one violation each, and the other two had two violations each [44].

Table 2. 2D Structures of compounds from *B. aristata*, *B. Monnieri*, *P. kurroa*, and *T. officinale*.

Compounds	2-D structures
	<i>Berberis aristata</i>
Berbamine	 <p>The chemical structure of Berbamine is a complex polycyclic alkaloid. It features a central piperazine ring system fused to two benzene rings. Each benzene ring is substituted with a methoxy group and a piperidine ring. The piperidine rings are further substituted with a benzyl group and a methoxy group. The structure is highly symmetrical and contains multiple nitrogen atoms.</p>
Berberine	 <p>The chemical structure of Berberine is a pentacyclic alkaloid. It consists of a central piperazine ring fused to two benzene rings. One of the benzene rings is substituted with a methoxy group and a piperidine ring. The piperidine ring is further substituted with a benzyl group and a methoxy group. The structure is highly symmetrical and contains multiple nitrogen atoms.</p>
Jatrorrhizine	 <p>The chemical structure of Jatrorrhizine is a pentacyclic alkaloid. It consists of a central piperazine ring fused to two benzene rings. One of the benzene rings is substituted with a methoxy group and a piperidine ring. The piperidine ring is further substituted with a benzyl group and a methoxy group. The structure is highly symmetrical and contains multiple nitrogen atoms.</p>
Meratin	 <p>The chemical structure of Meratin is a complex polycyclic alkaloid. It features a central piperazine ring system fused to two benzene rings. Each benzene ring is substituted with a methoxy group and a piperidine ring. The piperidine rings are further substituted with a benzyl group and a methoxy group. The structure is highly symmetrical and contains multiple nitrogen atoms.</p>
Oxyacanthine	 <p>The chemical structure of Oxyacanthine is a complex polycyclic alkaloid. It features a central piperazine ring system fused to two benzene rings. Each benzene ring is substituted with a methoxy group and a piperidine ring. The piperidine rings are further substituted with a benzyl group and a methoxy group. The structure is highly symmetrical and contains multiple nitrogen atoms.</p>
Palmatine	 <p>The chemical structure of Palmatine is a pentacyclic alkaloid. It consists of a central piperazine ring fused to two benzene rings. One of the benzene rings is substituted with a methoxy group and a piperidine ring. The piperidine ring is further substituted with a benzyl group and a methoxy group. The structure is highly symmetrical and contains multiple nitrogen atoms.</p>

Compounds	2-D structures
Rutin	 <p>The chemical structure of Rutin is a flavonoid glycoside. It consists of a flavanone core (quercetin) with a rhamnosyl group attached to the 3-position and a galactosyl group attached to the 7-position.</p>
<i>Bacopa Monnieri</i>	
Apigenin 7-glucuronide	 <p>The chemical structure of Apigenin 7-glucuronide shows a flavone core (apigenin) with a glucuronide group attached to the 7-position of the A-ring.</p>
D-mannitol	 <p>The chemical structure of D-mannitol is a polyhydroxy alcohol, specifically a six-carbon chain with hydroxyl groups at the 2, 3, 4, and 5 positions and primary hydroxyl groups at the 1 and 6 positions.</p>
L-aspartic acid	 <p>The chemical structure of L-aspartic acid is an amino acid with a central alpha-carbon bonded to a hydrogen atom, an amino group, and two carboxylate groups.</p>
Loliolide	 <p>The chemical structure of Loliolide is a bicyclic sesquiterpene lactone, featuring a decalin core with a lactone ring fused to one of the decalin rings.</p>
Luteolin	 <p>The chemical structure of Luteolin is a flavone with hydroxyl groups at the 5, 7, and 8 positions of the A-ring and at the 3 and 4 positions of the B-ring.</p>
Rosavin	 <p>The chemical structure of Rosavin is a stilbenoid glycoside, consisting of a stilbenoid core with a rhamnosyl group attached to the 3-position and a galactosyl group attached to the 7-position.</p>
<i>Picrorhiza kurroa</i>	
Androsin	 <p>The chemical structure of Androsin is a flavone glycoside, featuring a flavone core with a rhamnosyl group attached to the 3-position and a galactosyl group attached to the 7-position.</p>
Cucurbitacin B	 <p>The chemical structure of Cucurbitacin B is a complex polycyclic triterpene, characterized by a cucurbitane skeleton with multiple methyl and acetyl groups.</p>

Compounds	2-D structures
Cucurbitacin D	
Ferulic acid	
Picein	
Picoside I	
Picoside II	
Picoside III (6-feruloylcatalpol)	
Vanillic acid	
Veronicoside	

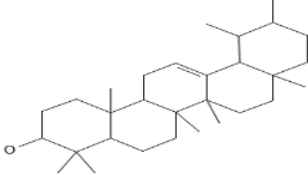
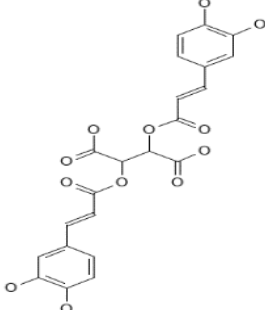
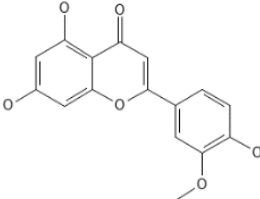
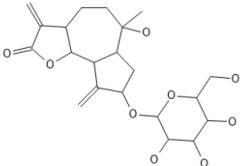
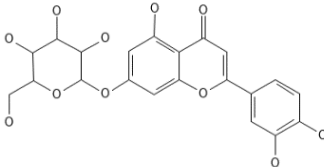
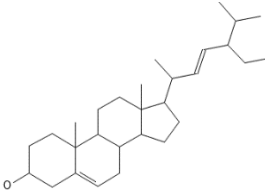
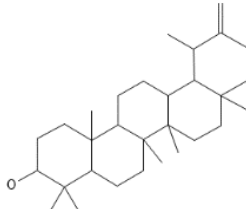
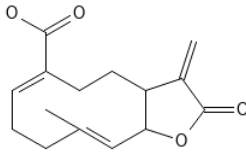
Compounds	2-D structures
<i>Taraxacum officinale</i>	
α -amyrin	
Chicoric acid	
Chrysoeriol	
Ixerin D	
Luteolin-7-glucoside	
Stigmasterol	
Taraxasterol	
Taraxinic acid	

Table 3. Computed physicochemical properties of screened compounds from *B. aristata*, *B. Monnieri*, *P. kurroa*, and *T. officinale*.

Compounds	PubChem Id	MW (g/mol)	H Bond Donor	H Bond Acceptor	TPSA (Å ²)	Log P (iLOGP)	Violations	Bioavailability score
<i>Berberis aristata</i>								
Berberine	275182	608.72	1	8	72.86	4.92	1	0.55
Berberine	2353	336.36	0	4	40.8	0	0	0.55
Jatrorrhizine	72323	338.38	1	4	51.8	-0.15	0	0.55
Meratin	122361330	626.52	11	17	289.66	0.9	3	0.17
Oxyacanthine	442333	608.72	1	8	72.86	4.69	1	0.55
Palmatine	19009	352.4	0	4	40.8	0.1	0	0.55
Rutin	5280805	610.52	10	16	269.43	1.58	3	0.17
<i>Bacopa Monnieri</i>								
Apigenin 7-glucuronide	5319484	446.36	6	11	187.12	1.53	2	0.11
D-mannitol	6251	182.17	6	6	121.38	0.34	1	0.55
L-aspartic acid	5960	133.1	3	5	100.62	-0.14	0	0.56
Loliolide	100332	196.24	1	3	46.53	1.88	1	0.55
Luteolin	5280445	286.24	4	6	111.13	1.86	0	0.55
Rosavin	9823887	428.43	6	10	158.3	2.19	1	0.55
<i>Picrorhiza kurroa</i>								
Androsin	164648	328.31	4	8	125.68	0.83	1	0.55
Cucurbitacin B	52813160	558.7	3	8	138.2	3.45	1	0.55
Cucurbitacin D	5281318	516.67	4	7	132.13	2.35	1	0.55
Ferulic acid	445858	194.18	2	4	66.76	1.62	0	0.85
Picein	92123	298.29	4	7	116.45	1.25	0	0.55
Picoside I	6440892	492.47	5	11	167.67	2.24	1	0.55
Picoside II	45358143	512.46	6	13	197.13	2.35	3	0.17
Picoside III (6-feruloylcatalpol)	24121289	538.5	6	13	197.13	1.37	3	0.17
Vanillic acid	8468	168.15	2	4	66.76	1.4	0	0.85
Veronicoside	13848081	466.44	5	11	167.67	1.18	1	0.55
<i>Taraxacum officinale</i>								
α-amyrin	73170	426.72	1	1	20.23	4.77	1	0.55
Chicoric acid	5281764	474.37	6	12	208.12	1	2	0.11
Chrysoeriol	5280666	300.26	3	6	100.13	2.44	0	0.55
Ixerin D	102000000	426.46	5	9	145.91	2.37	0	0.55
Luteolin-7-glucoside	5280637	448.38	7	11	190.28	1.83	2	0.17
Stigmasterol	5280794	412.69	1	1	20.23	5.01	1	0.55
Taraxasterol	115250	426.72	1	1	20.23	4.8	1	0.55
Taraxinic acid	157000000	262.3	1	4	63.6	1.89	0	0.85

3.2. Bioavailability radar.

This radar considers six physicochemical properties: size, polarity, lipophilicity, solubility, flexibility, and saturation. The pink area on the radar represents the optimal physicochemical space in which the molecule must fall to be classified as drug-like i.e., including polarity (TPSA between 20 and 130 Å²), size (MW between 150 and 500 g/mol), lipophilicity (XLOGP3 between -0.7 and +5.0), solubility (log S not exceeding six), flexibility (no more than nine rotatable bonds), and saturation (fraction of carbons in sp³ hybridization not less than 0.25) [45]. Table 3 (supplementary materials) displays the bioavailability radar analysis, which quickly assesses a molecule's drug-like properties. In *Berberis aristata*, two compounds showed bioavailability scores of 0.17, while five compounds showed scores of 0.55. In *Bacopa Monnieri*, one compound showed a bioavailability score of 0.11, while four compounds showed 0.55, and the other compound showed 0.56. In *Picrorhiza kurroa*, two

compounds showed a bioavailability score of 0.17, while six compounds showed 0.55, and the other two compounds showed 0.85. In *Taraxacum officinale*, one compound showed a bioavailability score of 0.11, while one compound showed 0.17, five compounds showed 0.55, and the other one compound showed 0.85.

3.3. Molecular docking.

In the field of structural molecular biology and computer-assisted drug design, molecular docking is a crucial tool. Ligand-protein docking aims to anticipate the primary binding mode(s) of a ligand with a protein with a known three-dimensional structure [46]. Through molecular docking-based virtual screening, a compound called Berbamine from *Berberis aristata*, Luteolin from *Bacopa Monnieri*, Cucurbitacin D from *Picrorhiza kurroa* and α -amyrin from *Taraxacum officinale* was identified as the best hit with a MolDock score of -8.04, -7.28, -7.78 and -9.02 kcal/mol respectively. Table 4 shows the docking score of compounds derived from *Berberis aristata*, *Bacopa Monnieri*, *Picrorhiza kurroa*, and *Taraxacum officinale* with 4ZXT.

Table 4. Docking score of compounds derived from *B. aristata*, *B. Monnieri*, *P. kurroa*, and *T. officinale* with a complex of ERK2 with catechol (PDB: 4ZXT).

Compounds	Binding energy (ΔG) (kcal/mol)	Ligand efficiency	Inhibition constant (μM)	Intermolecular energy (kcal/mol)	Vdw H-bond desolvation (kcal/mol)
<i>Berberis aristata</i>					
Berbamine	-8.04	-0.18	1.28	-9.23	-8.32
Berberine	-7.83	-0.31	1.81	-8.43	-7.92
Jatrorrhizine	-6.61	-0.26	14.38	-7.8	-7.05
Meratin	-3.77	-0.09	1.71	-9.14	-8.72
Oxyacanthine	-7.1	-0.16	6.25	-8.29	-6.26
Palmatine	-7.4	-0.28	3.79	-8.59	-7.95
Rutin	-5.83	-0.14	53.3	-10.6	-9.47
<i>Bacopa Monnieri</i>					
Apigenin 7-glucuronide	-7.34	-0.23	4.19	-10.32	-9.01
D-mannitol	-3.19	-0.27	4.63	-6.47	-6.27
L-aspartic acid	-4.31	-0.48	697.62	-6.1	-3.08
Loliolide	-6.59	-0.47	14.71	-6.89	-6.54
Luteolin	-7.28	-0.35	4.58	-8.78	-8.27
Rosavin	-5.88	-0.2	48.76	-9.76	-9.47
<i>Picrorhiza kurroa</i>					
Androsin	-5.63	-0.24	74.78	-8.31	-7.64
Cucurbitacin B	-6.78	-0.17		10.73	-9.46
Cucurbitacin D	-7.78	-0.21	1.99	-10.16	9.67
Ferulic acid	-6.37	-0.46	21.37	-7.86	-7.18
Picein	-6.09	-0.29	34.18	-8.48	-8.3
Picroside I	-5.37	-0.15	115.96	-9.25	-8.98
Picroside II	-4.52	-0.13	486.02	-8.7	-8.07
Picroside III (6-feruloylcatalpol)	-5.27	-0.14	137.35	-9.74	-9.55
Vanillic acid	-5.34	-0.45	122.66	-6.53	-5.73
Veroncoside	-6.31	-0.19	23.9	-9.88	-9.47
<i>Taraxacum officinale</i>					
α -amyrin	-9.02	-0.29	246.15	-9.31	-9.26
Chicoric acid	-6.7	-0.2	12.31	-11.77	-9.27
Chrysoeriol	-7.15	-0.33	5.77	-8.64	-8.31
Ixerin D	-6.71	-0.22	12.11	-9.09	-8.47
Luteolin-7-glucoside	-6.63	-0.21	13.75	-9.91	-9.77
Stigmasterol	-7.97	-0.27	1.44	-9.76	-9.77
Taraxasterol	-9.4	-0.3	129.15	-9.7	-9.65
Taraxinic acid	-6.99	-0.37	7.48	-7.59	-6.19

3.4. Interactions.

It was found that 2D ligand interactions from the compounds found in *B. aristata*, *B. Monnieri*, *P. kurroa*, and *T. officinale* when interacting with the Complex of ERK2 with catechol at the catalytically active site [47]. The compound Berbamine from *Berberis aristata* has a total of 6 van der Waals interactions at LYS330, ASP332, PHE331, ALA171, TYR205 and LYS203; 2 conventional hydrogen bond interactions at MET333 and VAL173; 1 carbon hydrogen bond interaction at ASP175; 1 pi-anion interaction at GLU334; 1 pi-sigma interaction at HIS178; and 1 pi-alkyl interaction at ARG172. The compound Luteolin from *Bacopa Monnieri* has a total of 5 van der Waals interactions at LYS330, PHE329, TYR139, ALA327, and PHE78; 3 conventional hydrogen bond interactions at PRO328, GLU326 and ARG77; 1 pi-pi T-shaped interaction at PHE331; and 1 pi-alkyl interaction at ALA325. The compound Cucurbitacin D from *Picrorhiza kurroa* has a total of 13 van der Waals interactions at SER153, LYS114, GLY32, ILE31, VAL39, MET108, LEU156, ALA52, ILE84, LYS54, CME166, GLY34 and TYR113; and 3 conventional hydrogen bond interactions at ASP111, GLU33 and GLN105. The compound α -amyrin from *Taraxacum officinale* has a total of 14 van der Waals interactions at ASP167, CME166, SER153, GLU33, LYS114, ASP111, LEU156, THR110, LEU107, ASP106, ALA52, ILE31, VAL39, GLY34; 1 conventional hydrogen bond interaction at MET108; and 1 alkyl interaction at ALA35 as shown in Table 5 (Supplementary materials).

4. Conclusions

The article delves into the intricate field of phytochemistry, which studies the diverse range of bioactive compounds found in medicinal plants. These phytochemicals are crucial for developing natural remedies and pharmaceuticals. Docking, a computational technique, plays a significant role in this process by filtering vast libraries of chemical compounds, ranking their effectiveness, and proposing structural hypotheses on how they interact with biological targets. This technique is instrumental in refining lead compounds to enhance their efficacy and safety. Despite its potential, only a limited number of researchers have explored the application of docking against various cancer cell lines. However, those studies have shown considerable efficacy, particularly against lung cancer, indicating a promising avenue for cancer treatment. To develop effective clinical drugs, it is essential to evaluate each compound's bioavailability, toxicity, and structure-function relationship. This ensures that the compounds are effective and safe for human use. Beyond computational predictions, developing clinical drugs requires rigorous clinical trials and further research to understand the synergistic effects of different phytochemicals. Specifically, the article highlights the need to investigate compounds from plants like *B. aristata*, *B. Monnieri*, *P. kurroa*, and *T. officinale* to understand how they work together to enhance therapeutic effects. A deeper understanding of biological processes, action methods, and signal transduction pathways is necessary. This knowledge helps identify new therapeutic targets and refine existing treatments. In conclusion, the article underscores the importance of an integrated approach that combines phytochemistry, docking studies, bioavailability and toxicity assessments, and clinical trials. By advancing our understanding of the interactions and effects of phytochemicals, researchers can develop more effective and safer drugs to treat various diseases, including cancer.

Funding

This research received no external funding.

Acknowledgments

The author would like to express gratitude to their University for being a consistent source of support and for establishing the environment for research.

Conflicts of Interest

The authors state that there are no conflicts of interest.

References

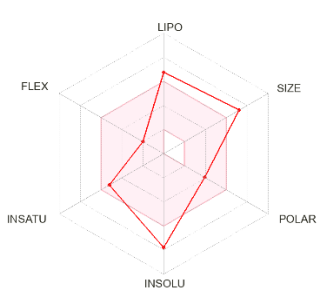
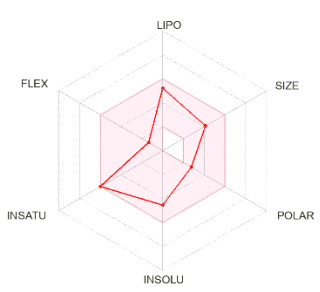
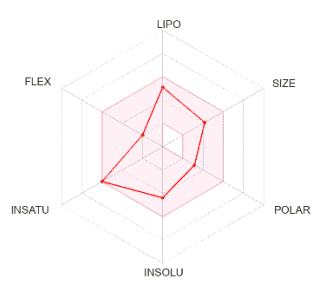
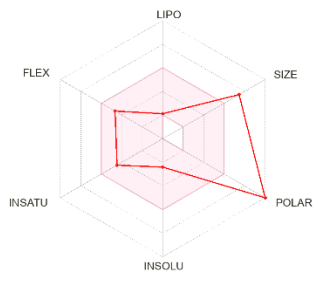
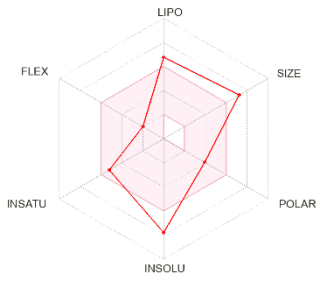
1. Johariya, V.; Joshi, A.; Malviya, N.; Malviya, S. Introduction to Cancer. In *Medicinal Plants and Cancer Chemoprevention*; CRC Press: **2024**; pp. 1-28.
2. Liu, L. U.; Xie, B.; Zhu, W.; He, Q.; Zhou, J.; Liu, S.; Tao, Y.; Xiao, D. High expression of PD-L1 mainly occurs in non-small cell lung cancer patients with squamous cell carcinoma or poor differentiation. *Oncology Research* **2023**, *31*, 275, <https://doi.org/10.32604/or.2023.028227>.
3. Park, J. A.; Suzuki, K. Novel Screening Tools for Lung Cancer. *Thoracic Surgery Clinics* **2023**, *33*, 215-226, <https://doi.org/10.1016/j.thorsurg.2023.04.011>.
4. Kour, O.; Garg, M. The genomic landscape of lung adenocarcinoma—insights towards personalized medicine. *Proceedings of the Indian National Science Academy* **2021**, *87*, 562-577, <https://doi.org/10.1007/s43538-021-00054-1>.
5. De Mello, R. A.; Neves, N. M.; Tadokoro, H.; Amaral, G. A.; Castelo-Branco, P.; Zia, V. A. D. A. New target therapies in advanced non-small cell lung cancer: a review of the literature and future perspectives. *Journal of Clinical Medicine* **2020**, *9*, 3543, <https://doi.org/10.3390/jcm9113543>.
6. Wu, M.; Jiang, J.; Zhang, X.; Chen, J.; Chang, Q.; Chen, R. RT-based combination therapy for brain metastasis from NSCLC with non-EGFR mutation/ALK gene rearrangement: A network meta-analysis. *Frontiers in Oncology* **2022**, *12*, 1024833, <https://doi.org/10.3389/fonc.2022.1024833>.
7. Jahan, F.; Alvi, S. S.; Islam, M. H. *Berberis aristata* and its secondary metabolites: Insights into nutraceutical and therapeutical applications. *Pharmacological Research-Modern Chinese Medicine* **2022**, *5*, 100184, <https://doi.org/10.1016/j.prmcm.2022.100184>.
8. Bhardwaj, D.; Kaushik, N. HPLC–DAD fingerprinting coupled with chemometric analysis can successfully differentiate Indian *Berberis* species and its plant parts. *3 Biotech* **2023**, *13*, 254, <https://doi.org/10.1007/s13205-023-03644-6>.
9. Rawat, S.; Goswami, R.; Ambwani, S.; Ambwani, T. K. Exploring the immunomodulatory and antioxidant capacities of *Berberis aristata* in avian lymphocytes. *The Journal of Phytopharmacology* **2024**, *13*, 254-260, <https://doi.org/10.31254/phyto.2024.13310>.
10. Kaur, R.; Urvashi; Kumar, A. Species of the *Berberis* Genus Found in the Western Himalayas. In *Immunity Boosting Medicinal Plants of the Western Himalayas*, Sharma, A., Nayik, G.A., Eds.; Springer Nature Singapore: Singapore, **2023**; pp. 107-143, https://doi.org/10.1007/978-981-19-9501-9_5.
11. Emran, T. B.; Rahman, M. A.; Uddin, M. M. N.; Dash, R.; Hossen, M. F.; Mohiuddin, M.; Alam, M. R. Molecular docking and inhibition studies on the interactions of *Bacopa monnieri*'s potent phytochemicals against pathogenic *Staphylococcus aureus*. *DARU Journal of Pharmaceutical Sciences* **2015**, *23*, 1-8, <https://doi.org/10.1186/s40199-015-0106-9>.
12. Banerjee, S.; Anand, U.; Ghosh, S.; Ray, D.; Ray, P.; Nandy, S.; Deshmukh, G. D.; Tripathi, V.; Dey, A. Bacosides from *Bacopa monnieri* extract: An overview of the effects on neurological disorders. *Phytotherapy Research* **2021**, *35*, 5668-5679, <https://doi.org/10.1002/ptr.7203>.
13. Gouthami, N. S.; Jain, S. K.; Jain, N. K.; Wadhwan, N.; Agrawal, C.; Panwar, N. L. Exploring the Nutraceutical Effects of Brahmi (*Bacopa monnieri*) in Agriculture: Potential Applications and Benefits. *Environment and Ecology* **2023**, *41*, 2947-2954, <https://doi.org/10.60151/envec/PZST7159>.

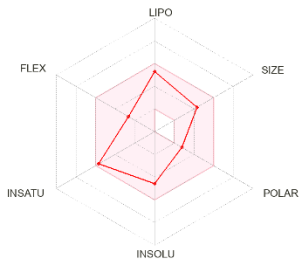
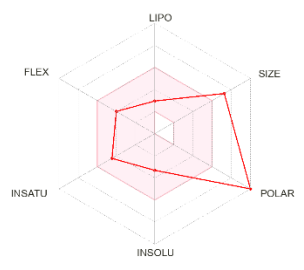
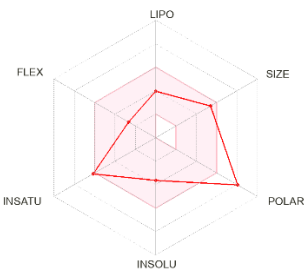
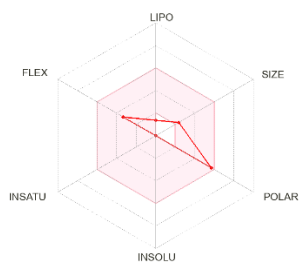
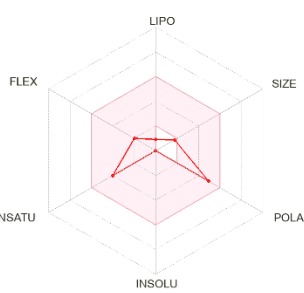
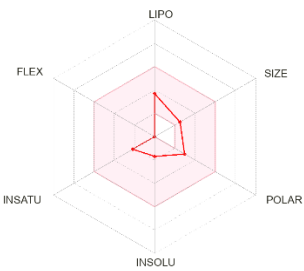
14. Agarwal, A.; Mishra, B.; Gupta, A.; Srivastava, M. V. P.; Basheer, A.; Sharma, J.; Vishnu, V. Y. Importance of high-quality evidence regarding the use of *Bacopa monnieri* in dementia. *Frontiers in aging neuroscience* **2023**, *15*, 1134775, <https://doi.org/10.3389/fnagi.2023.1134775>.
15. Nishanth, B. J.; Vijayababu, P.; Kurian, N. K. *Bacopa monnieri* Extract As a Neuroprotective and Cognitive Enhancement Agent. *International Journal of Drug Discovery and Pharmacology* **2023**, 44-56, <https://doi.org/10.53941/ijddp.2023.100015>.
16. Tabassam, Q.; Mehmood, T.; Ahmed, S.; Saeed, S.; Raza, A. R.; Anwar, F. GC-MS metabolomics profiling and HR-APCI-MS characterization of potential anticancer compounds and antimicrobial activities of extracts from *Picrorhiza kurroa* roots. *J. Appl. Biomed.* **2021**, *19*, 26-39, <https://doi.org/10.32725/jab.2020.017>.
17. Masood, M.; Arshad, M.; Rahmatullah, Q.; Sabir, S.; Shoaib, M.; Amjad, H. Q.; Tahir, Z. *Picrorhiza kurroa*: An ethnopharmacologically important plant species of Himalayan region. *Pure and Applied Biology (PAB)* **2021**, *4*, 407-417, <http://dx.doi.org/10.19045/bspab.2015.43017>.
18. Soni, D.; Wahi, D.; Verma, S. In vitro study on anti-proliferative and anti-cancer activity of picrosides in triple-negative breast cancer. *Medical Oncology* **2024**, *41*, 1-10, <https://doi.org/10.1007/s12032-024-02397-3>.
19. Kaur, K.; Kaur, G.; Singh, V. *Picrorhiza kurroa* Royle ex Benth.: Kutki. Immunity Boosting Medicinal Plants of the Western Himalayas **2023**, 335-370, https://doi.org/10.1007/978-981-19-9501-9_15.
20. Soni, D.; Grover, A. "Picrosides" from *Picrorhiza kurroa* as potential anti-carcinogenic agents. *Biomedicine & Pharmacotherapy* **2019**, *109*, 1680-1687, <https://doi.org/10.1016/j.biopha.2018.11.048>.
21. Di Napoli, A.; Zucchetti, P. A comprehensive review of the benefits of *Taraxacum officinale* on human health. *Bulletin of the National Research Centre* **2021**, *45*, 1-7, <https://doi.org/10.1186/s42269-021-00567-1>.
22. Nazeam, J. A.; El-Emam, S. Z. Middle Eastern Plants with Potent Cytotoxic Effect Against Lung Cancer Cells. *Journal of Medicinal Food* **2024**, *27*, 198-207, <https://doi.org/10.1089/jmf.2022.0098>.
23. Tiwari, D.; Kewlani, P.; Singh, L.; Rawat, S.; Bhatt, I. D.; Sundriyal, R. C.; Pande, V. A review on natural bioactive compounds of *Taraxacum officinale* Weber: A potential anticancer plant. *RPS Pharmacy and Pharmacology Reports* **2024**, *3*, <https://doi.org/10.1093/rpsppr/rqae009>.
24. Roy, A.; Sharma, N.; Luthra, R. In-silico analysis of antiviral fungal inhibitors against Mpro receptor protein. *Vegetos* **2024**, <https://doi.org/10.1007/s42535-024-00915-2>.
25. Haque, B.; Gupta, A.; Roy, A. Green fabrication of Ag-Ni-Mn-Zn nanoparticles from watermelon peels and its antioxidant, dye degradation and molecular docking studies. *Clean Techn Environ Policy* **2024**, <https://doi.org/10.1007/s10098-024-02906-y>.
26. Kania-Dobrowolska, M.; Baraniak, J. Dandelion (*Taraxacum officinale* L.) as a source of biologically active compounds supporting the therapy of co-existing diseases in metabolic syndrome. *Foods* **2022**, *11*, 2858, <https://doi.org/10.3390/foods11182858>.
27. Bontha, L.; Kumar, P.; Dokala, A.; Pingili, D.; Putta, V. R.; kumar Vuradi, R.; Kotha, L. R. Synthesis, in-silico based virtual screening, anti-cancer potential of novel 1, 2, 3-triazole-thiadiazole hybrid derivatives as Aurora kinase A (ARK-A) and Extracellular regulated kinase 2 (ERK2) dual inhibitors. *Research Square* **2023**, *32*, 2419-2431, <https://doi.org/10.21203/rs.3.rs-2691747/v1>.
28. E Lohning, A.; M Levonis, S.; Williams-Noonan, B.; S Schweiker, S. A practical guide to molecular docking and homology modeling for medicinal chemists. *Current Topics in Medicinal Chemistry* **2017**, *17*, 2023-2040, <https://doi.org/10.2174/1568026617666170130110827>.
29. Gupta, A.; Haque, B.; Roy, A.; Malik, A.; Khan, A. A.; Kaur, K.; Roy, A. Antioxidant, dye degradation, and molecular docking studies of orange peel extract derived Ag-Fe-Ni nanoparticles. *Inorganic Chemistry Communications* **2024**, *166*, 112599, <https://doi.org/10.1016/j.inoche.2024.112599>.
30. Bennici, A.; Mannucci, C.; Calapai, F.; Cardia, L.; Ammendolia, I.; Gangemi, S.; Calapai, G.; Soler, D. Safety of Medical Cannabis in Neuropathic Chronic Pain Management. *Molecules* **2021**, *26*, 6257, <https://doi.org/10.3390/molecules26206257>.
31. Jemal, K. Molecular docking studies of phytochemicals of *Allophylus serratus* against cyclooxygenase-2 enzyme. *bioRxiv* **2019**, 866152, <https://doi.org/10.1101/866152>.
32. Roy, A.; Gupta, A.; Verma, D. Evaluation of different phytochemicals from *Cannabis sativa* against Myelin oligodendrocyte glycoprotein receptor. *Vegetos* **2023**, 1-11, <https://doi.org/10.1007/s42535-023-00753-8>.

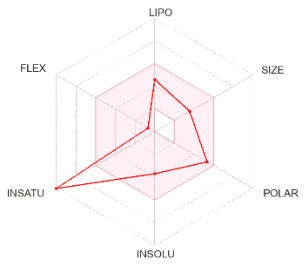
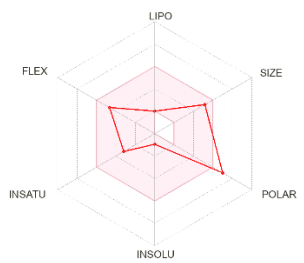
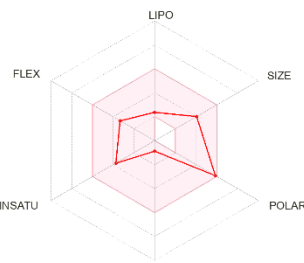
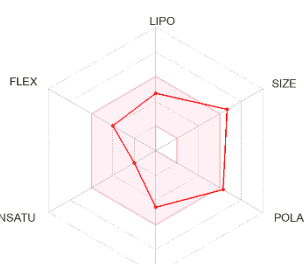
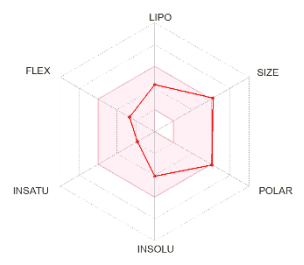
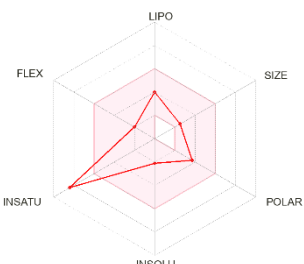
33. Gupta, A.; Roy, A.; Pandit, S.; Pandey, N.; Rustagi, S. Evaluation of bioactive compounds obtained from ginkgo biloba against crystal structure of myelin oligodendrocyte glycoprotein (MOG). *OBM Neurobiology* **2023**, *7*, 1-34, <https://doi.org/10.21926/obm.neurobiol.2304186>.
34. Gupta, A.; Roy, A.; Raja, V.; Rustagi, S.; Malik, S.; Verma, D. In-silico studies of phytoconstituents of *Bacopa monnieri* and *Centella asiatica* with Crystal structure of Myelin Oligodendrocyte Glycoprotein against primary demyelination in Multiple Sclerosis. *Journal of Integrated Science and Technology* **2024**, *12*, 764-764, <https://doi.org/10.62110/sciencein.jist.2024.v12.764>.
35. Gurjar, S. P.; Roy, A.; Gupta, A. Competitive inhibition of catechol from *Andrographis paniculata* in the complex of ERK2 in lung metastasis. *Journal of Integrated Science and Technology* **2024**, *12*, 719-719.
36. Gurjar, S.P.; Gupta, A.; Roy, A. Molecular docking studies of phytocompounds from *Artemisia monosperma* against ERK2 kinase in lung cancer. *Journal of Molecular Chemistry* **2023**, *3*, 591-591.
37. Sengupta, P.; Raman, S.; Chowdhury, R.; Lohitesh, K.; Saini, H.; Mukherjee, S.; Paul, A. Evaluation of apoptosis and autophagy inducing potential of *Berberis aristata*, *Azadirachta indica*, and their synergistic combinations in parental and resistant human osteosarcoma cells. *Frontiers in oncology* **2017**, *7*, 296, <https://doi.org/10.3389/fonc.2017.00296>.
38. Zaib, S.; Saeed Shah, H.; Usman, F.; Shahzadi, K.; Mazhar Asjad, H.; Khan, R.; Dera, A. A.; Pashameah, R. A.; Alzahrani, E.; Farouk, A.; Khan, I. Green Synthesis of Gelatin-Lipid Nanocarriers Incorporating *Berberis aristata* Extract for Cancer Therapy; Physical Characterization, Pharmacological and Molecular Modeling Analysis. *ChemistrySelect* **2022**, *7*, e202203430, <https://doi.org/10.1002/slct.202203430>.
39. Moskwa, J.; Naliwajko, S. K.; Markiewicz-Żukowska, R.; Gromkowska-Kępką, K. J.; Nowakowski, P.; Strawa, J. W.; Borawska, M. H.; Tomczyk, M.; Socha, K. Chemical composition of Polish propolis and its antiproliferative effect in combination with *Bacopa monnieri* on glioblastoma cell lines. *Scientific Reports* **2020**, *10*, 21127, <https://doi.org/10.1038/s41598-020-78014-w>.
40. Fatima, U.; Roy, S.; Ahmad, S.; Al-Keridis, L. A.; Alshammari, N.; Adnan, M.; Islam, A.; Hassan, M. I. Investigating neuroprotective roles of *Bacopa monnieri* extracts: Mechanistic insights and therapeutic implications. *Biomedicine & Pharmacotherapy*, **2022**, *153*, 113469, <https://doi.org/10.1016/j.biopha.2022.113469>.
41. Almeleebia, T. M.; Alsayari, A.; Wahab, S. Pharmacological and Clinical Efficacy of *Picrorhiza kurroa* and Its Secondary Metabolites: A Comprehensive Review. *Molecules* **2022**, *27*, 8316, <https://doi.org/10.3390/molecules27238316>.
42. Nassan, M. A.; Soliman, M. M.; Ismail, S. A.; El-Shazly, S. Effect of *Taraxacum officinale* extract on PI3K/Akt pathway in DMBA-induced breast cancer in albino rats. *Bioscience Reports*, **2018**, *38*, BSR20180334, <https://doi.org/10.1042/BSR20180334>.
43. Liu, L.; Xiong, H.; Ping, J.; Ju, Y.; Zhang, X. *Taraxacum officinale* protects against lipopolysaccharide-induced acute lung injury in mice. *Journal of Ethnopharmacology* **2010**, *130*, 392-397, <https://doi.org/10.1016/j.jep.2010.05.029>.
44. Butina, D.; Segall, M. D.; Frankcombe, K. Predicting ADME properties *in-silico*: methods and models. *Drug Discovery Today* **2002**, *7*, S83-S88, [https://doi.org/10.1016/S1359-6446\(02\)02288-2](https://doi.org/10.1016/S1359-6446(02)02288-2).
45. Ekins, S.; Lane, T. R.; Urbina, F.; Puhl, A. C. *In-silico* ADME/tox comes of age: Twenty years later. *Xenobiotica* **2023**, 1-7, <https://doi.org/10.1080/00498254.2023.2245049>.
46. Daina, A.; Michielin, O.; Zoete, V. SwissADME: a free web tool to evaluate pharmacokinetics, drug-likeness and medicinal chemistry friendliness of small molecules. *Scientific Reports* **2017**, *7*, 42717, <https://doi.org/10.1038/srep42717>.
47. Kishor, D.; Deweshri, N.; Vijayshri, R.; Ruchi, S.; Ujwala, M. Molecular Docking: Metamorphosis in Drug Discovery. In *Molecular Docking*, Erman Salih, I., Ed.; IntechOpen: Rijeka, **2022**; p. Ch. 3. <https://doi.org/10.5772/intechopen.105972>.

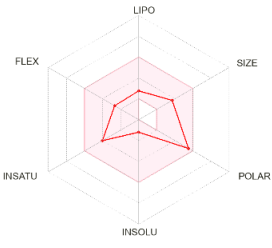
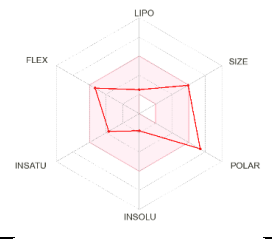
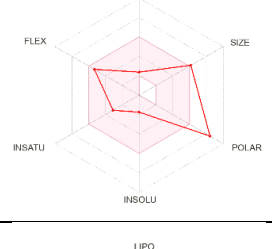
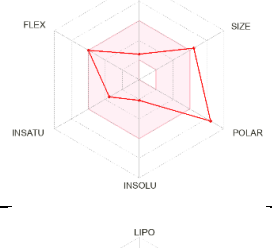
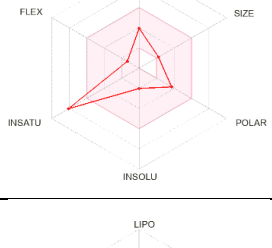
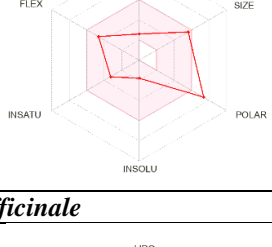
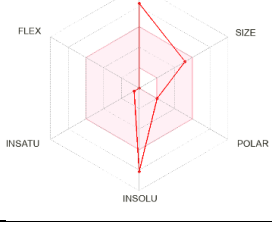
Supplementary materials

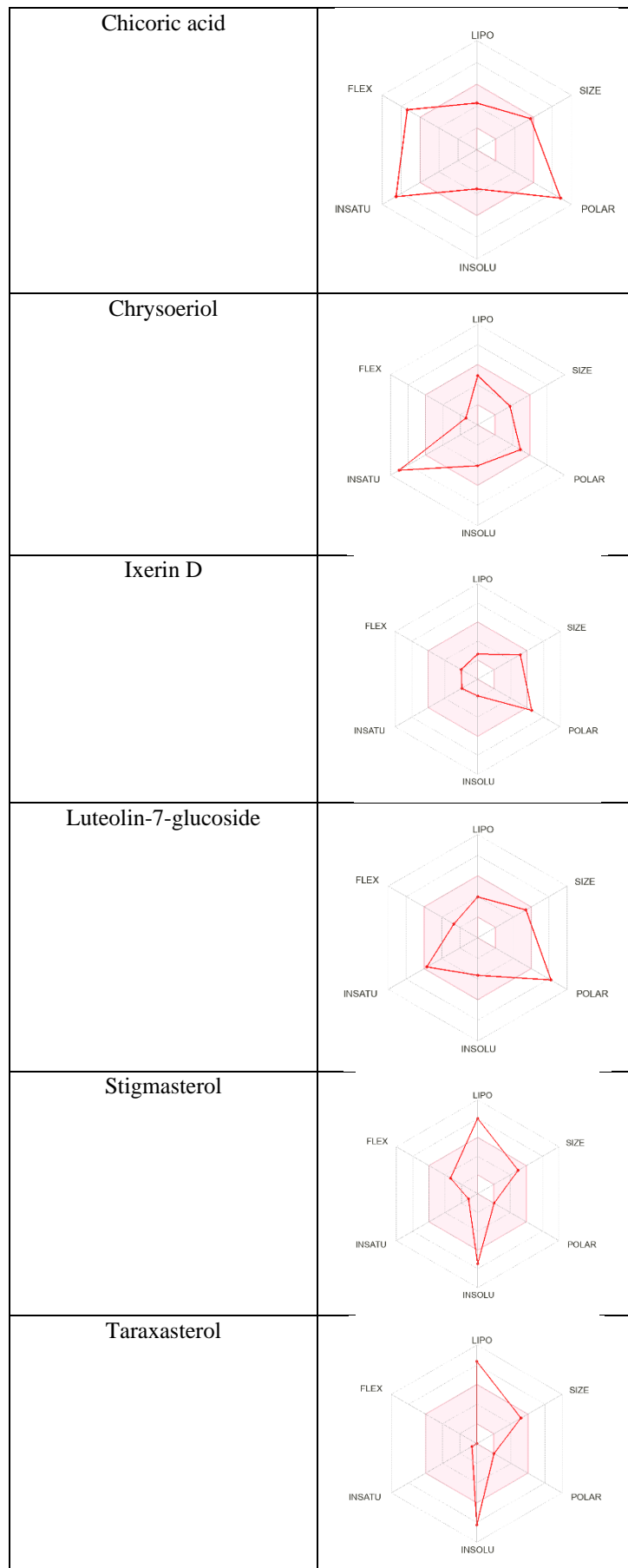
Table 3. Bioavailability Radar analysis of screened compounds from *B. aristata*, *B. Monnieri*, *P. kurroa* and *T. officinale* using SwissADME

Compounds	Bioavailability Radar
<i>Berberis aristata</i>	
Berbamine	
Berberine	
Jatrorrhizine	
Meratin	
Oxyacanthine	

<p>Palmatine</p>	
<p>Rutin</p>	
<p><i>Bacopa Monnieri</i></p>	
<p>Apigenin 7-glucuronide</p>	
<p>D-mannitol</p>	
<p>L-aspartic acid</p>	
<p>Loliolide</p>	

Luteolin	
Rosavin	
<i>Picrorhiza kurroa</i>	
Androsin	
Cucurbitacin B	
Cucurbitacin D	
Ferulic acid	

Picein	
Picroside I	
Picroside II	
Picroside III (6-feruloylcatalpol)	
Vanillic acid	
Veronicoside	
<i>Taraxacum officinale</i>	
α -amyrin	



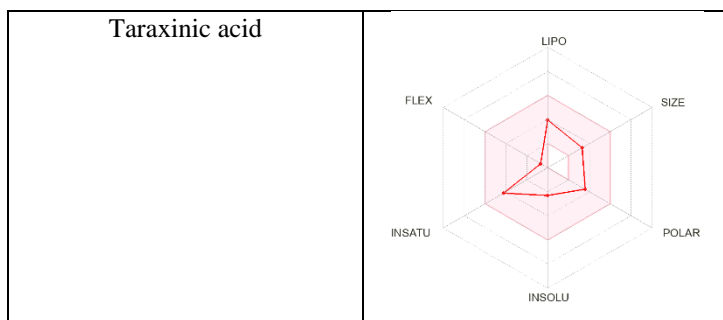
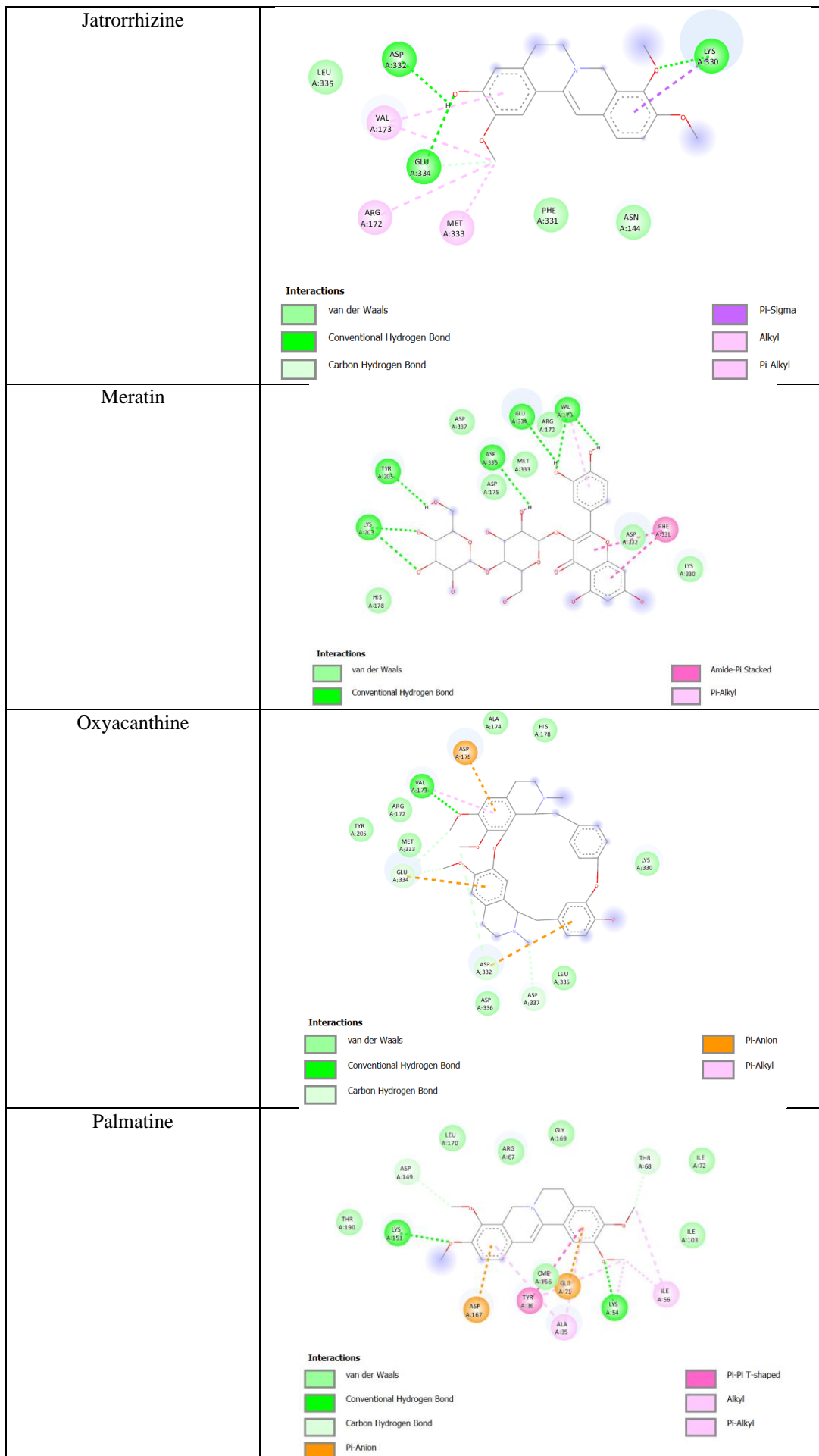
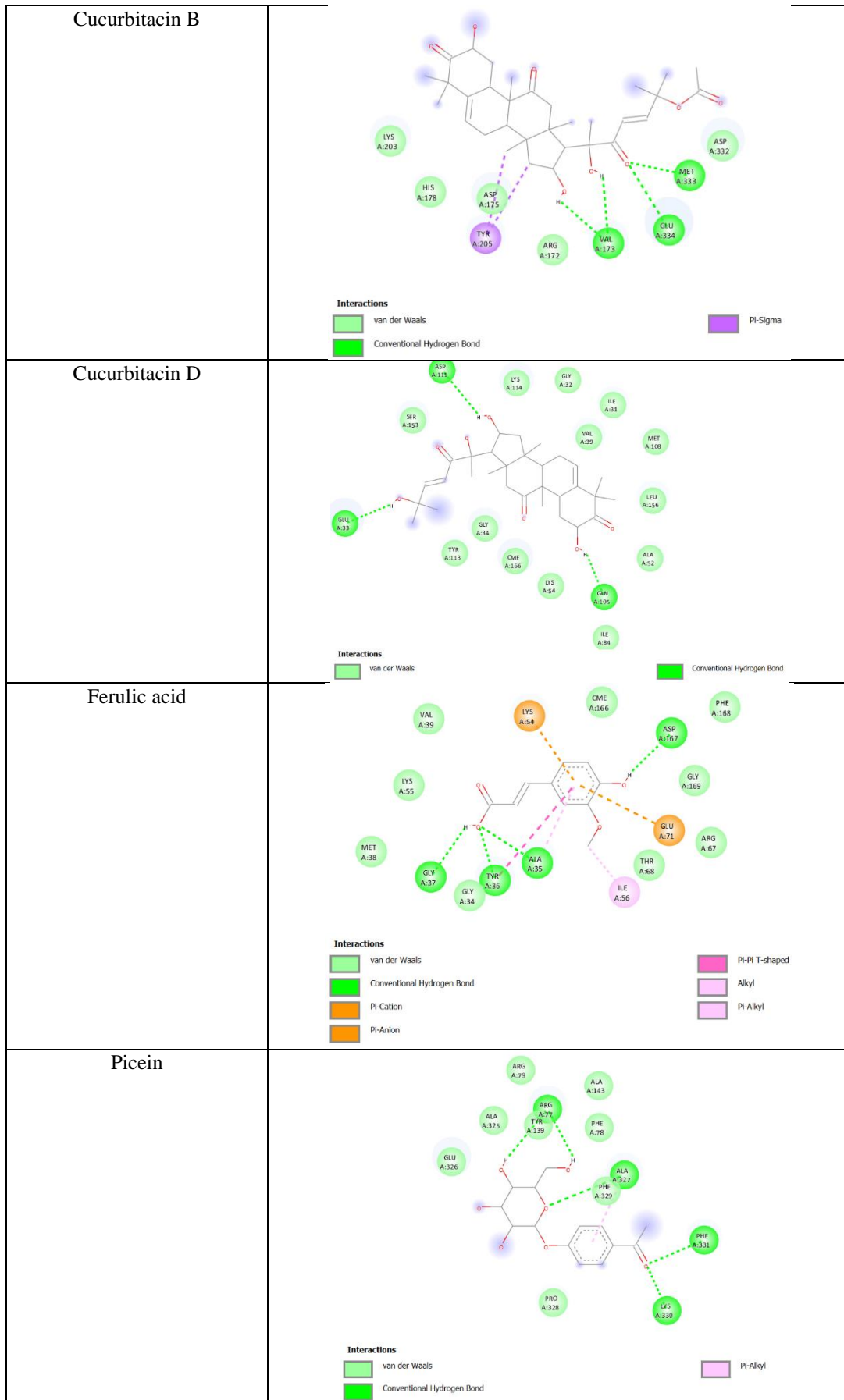


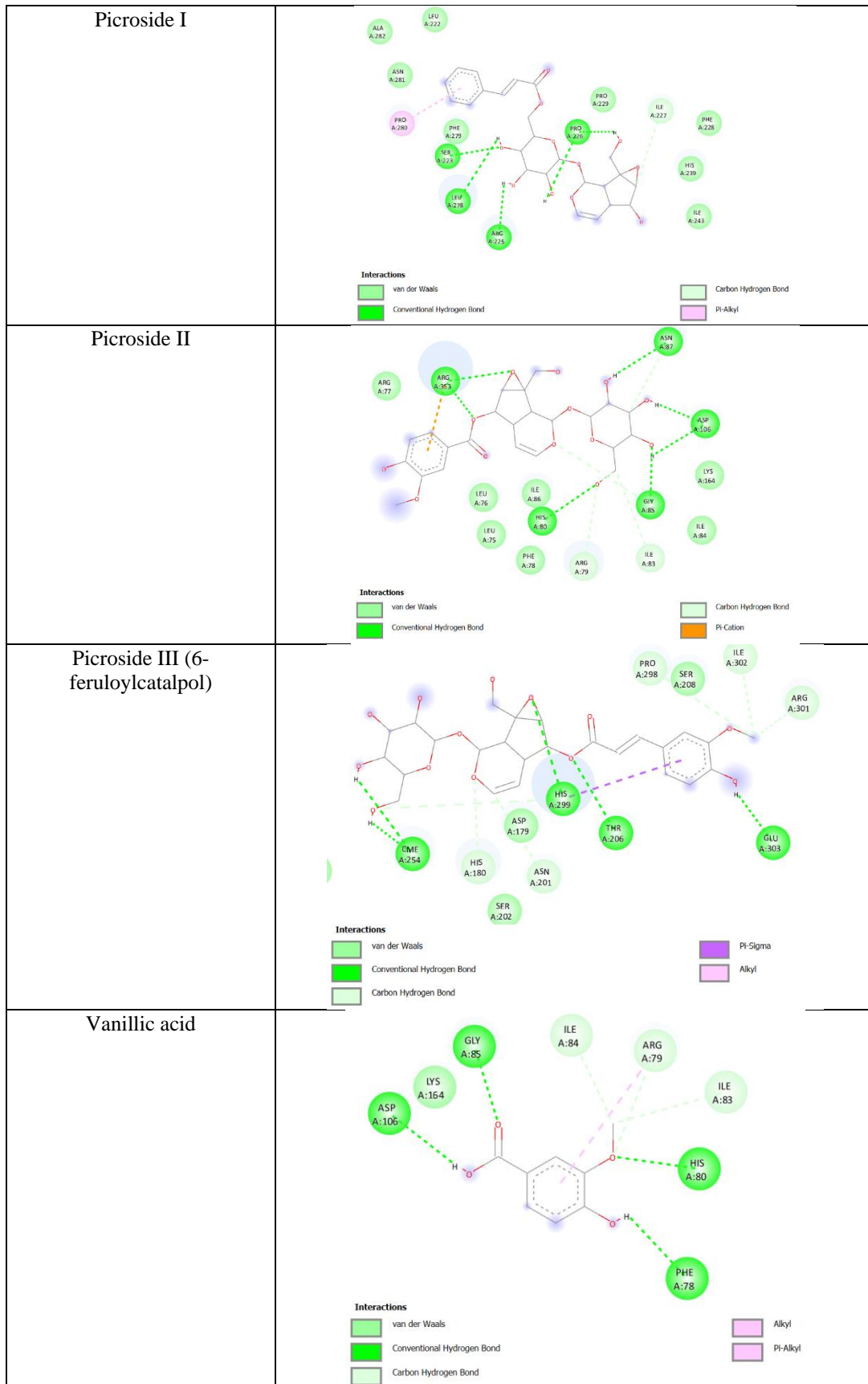
Table 5. Various 2D Ligand interactions generated by compounds of *B. aristata*, *B. Monnieri*, *P. kurroa* and *T. officinale* with Complex of ERK2 with catechol (PDB: 4ZXT) at the catalytically active site

Ligands	2D Ligand Interactions with 4ZXT
Berberis aristata	Berberis aristata
Berbamine	<p>Interactions</p> <ul style="list-style-type: none"> van der Waals Conventional Hydrogen Bond Carbon Hydrogen Bond Pi-Anion Pi-Sigma Pi-Alkyl
Berberine	<p>Interactions</p> <ul style="list-style-type: none"> van der Waals Conventional Hydrogen Bond Pi-Anion Pi-Pi T-shaped Alkyl Pi-Alkyl



<p>Loliolide</p>	
<p>Luteolin</p>	
<p>Rosavin</p>	
<p><i>Picrorhiza kurroa</i></p>	
<p>Androsin</p>	





<p>Ixerin D</p>	
<p>Luteolin-7-glucoside</p>	
<p>Stigmasterol</p>	
<p>Taraxasterol</p>	

